Received: 8 February 2018 | Revised: 25 May 2018 | Accepted: 25 May 2018

DOI: 10.1002/rcm.8181

RESEARCH ARTICLE

WILEY Rapid Communications in Mass Spectrometry

Benefits of NaCl addition for time-of-flight secondary ion mass spectrometry analysis including the discrimination of diacylglyceride and triacylglyceride ions

Sanna Sämfors[1] | Andrew G. Ewing[1,2] | John S. Fletcher[2]

[1] Department of Chemistry and Chemical Engineering, Chalmers University of Technology, 412 96 Gothenburg, Sweden

[2] Department of Chemistry and Molecular Biology, University of Gothenburg, 412 96 Gothenburg, Sweden

Correspondence
John S. Fletcher, Department of Chemistry and Molecular Biology, University of Gothenburg, 412 96 Gothenburg, Sweden.
Email: john.fletcher@chem.gu.se

Funding information
Foundation for the National Institutes of Health; Knut och Alice Wallenbergs Stiftelse; Vetenskapsrådet

Rationale: Diacylglycerides (DAGs) and triacylglycerides (TAGs) are two important lipid classes present in all mammalian cells that share similar chemical structures but differ in biological function in cells and tissues. Differentiation of these two species during time-of-flight secondary ion mass spectrometry (ToF-SIMS) analysis is therefore important, but has been difficult due to the formation of DAG-like ions during the ionization process of TAGs.

Methods: We investigated the use of salt adduct formation as a quick and simple method to determine the origin of the DAG-like ions in ToF-SIMS spectra. NaCl was added to lipid standards of a DAG and a TAG and differences in fragmentation patterns were identified. The salt was then applied to prepared tissue samples by spraying with a saturated solution of NaCl in methanol and samples were analysed with ToF-SIMS using a 40 keV $(CO_2)_{6k}^+$ primary ion beam.

Results: A 40 Da peak shift was observed in the DAG spectrum that was not observed in the TAG spectrum ($[M + H - H_2O]^+$ to $[M + Na]^+$) while the isobaric $[M - RCOO]^+$ peak did not shift allowing differentiation between the two species. Spraying NaCl on to tissue sections indicated that the DAG-like ions originated from TAGs.

Conclusions: With the method described in this paper, simple addition of salt by spraying on the sample leads to better interpretation of complex mass spectra from biological tissue samples, discriminating DAG and TAG fragment peaks.

1 | INTRODUCTION

Time-of-flight secondary ion mass spectrometry (ToF-SIMS) is a useful method for studying lipids due to the ionization and sputtering properties of lipid molecules. The use of energetic primary ions to eject secondary ions from a sample surface meant that for a long time SIMS fell into the hard ionization category, but advances in ion beam technology have led to the introduction of polyatomic (e.g. C_{60}^+) and now gas cluster (e.g. Ar_{4000}^+) ion beams that produce spectra that, while still containing many fragment species, also include much more signal from intact pseudo-molecular ions (normally $[M \pm H]^{\pm}$ and adduct species $[M + Na/K]^+$, etc.).[1] Advances in the mass analyser technology featured with SIMS instruments, either new types of ToF configuration[2] or hybrid instruments incorporating analysers normally associated with other types of MS,[3,4] have improved mass accuracy to several ppm or better – compared with around 150 ppm for large molecular peaks with conventional SIMS instruments.[5] MS/MS capabilities are now also available for several types of SIMS instruments with numerous studies appearing in the literature.[6-9] However, due to the high cost of replacing or upgrading SIMS instruments, the majority of the community is reliant on conventional systems where the complexity of biological samples combined with the complexity of imaging spectra makes peak identification difficult. In order to meet the demands associated with biological/clinical analysis, it is important that complex mass spectrometric data are accurately interpreted. Hence, new tools and methods that can be used for help with peak assignments, especially for biological samples, are needed.

Diacylglycerides (DAGs) and triacylglycerides (TAGs) are two major lipid classes that are present in all mammalian cells and most biological tissues where they serve as important components. They share similar structures but have different functions within the cell. DAGs are involved in a variety of metabolic pathways.[10] They are used as building blocks for glycerophospholipids and as components of cellular membranes.[11] Another important function for DAGs is as signalling molecules when they act as lipid secondary messengers.[12,13] DAGs can be derived either through hydrolysis of phospholipids via specific enzymes that cleave the intact lipids or from *de novo* synthesis.[10] The accumulation of DAGs has been shown to be associated with diabetes,[14] carcinoma[15] and coronary heart disease.[16] In contrast, the main function of TAGs is to serve as energy storage.[17,18] TAGs are stored in lipid droplets within the cell and are used by the cell as energy or as a source of DAGs.[19] Since TAGs and DAGs exhibit different functions within a cell, it is important to be able to distinguish these two from each other during lipidomic analysis of different samples to obtain useful biological information that connects to the physiological differences between different samples.

A problem when analysing DAG and TAG species with ToF-SIMS is that it is difficult to distinguish between these species due to the formation of DAG-like ions via the fragmentation of TAG species during the ionization process. The DAG-like ions originating from a TAG species are isobaric with native DAG species, making the distinction between these species impossible without MS/MS.[20] Although there is evidence that the amounts of DAGs are lower in many tissues compared to TAGs,[21-23] many ToF-SIMS studies identify these DAG-like ions as DAG species although it is more likely that the peaks arise from fragmentation of TAG species. Similar problems have been detected in other mass spectrometric methods such as matrix-assisted laser desorption/ionization (MALDI), where the formation of pseudo-DAG fragments can also be observed.[24,25] Studies using MALDI have led to speculation that DAG-like ions come from post-source reformation of unstable protonated TAGs.[26] In another study, Gidden et al. used the addition of a base to the matrix to stop the formation of the protonated TAG and, therefore, the formation of the DAG-like ions.[27] In SIMS, the ion generation process is different from that in MALDI, so to prevent the formation of the DAG-like ions a different approach is needed. Cations such as sodium are thought to interact with the oxygen on the carboxylic groups of the fatty acid chains altering the electron density, hence influencing fragmentation.[28]

In the work reported in this paper, the use of salt addition to a sample to form distinctive fragmentation patterns for the DAG and TAG species by formation of salt adduct ions (e.g. $[M + Na]^+$) is investigated. This allows determination of the species class from which the peak originates. The proposed method uses a simple setup for application of salt, and interpretation of spectra is performed without the need for MS/MS capabilities on the SIMS instrument. Salt was first added to lipid standards of a DAG and a TAG and the fragmentation patterns were evaluated. The salt was then applied to more complex biological tissues, and the general applicability of the method was determined with additional advantages or drawbacks assessed.

2 | EXPERIMENTAL

2.1 | Preparation of lipid standards

Lipid standards (Sigma-Aldrich, Sweden) were dissolved separately in chloroform to create lipid solutions. The lipid standards used were 1,2-dioleoyl-rac-glycerol (DAG) and 1,3-dioleoyl-2-palmitoylglycerol (TAG). For control samples, without salt addition, the lipid standard solution (1 mg/mL) was pipetted onto clean silicon wafers (30 min sonication in ethanol and then chloroform) and dried at room temperature in a fume hood. To ensure that the sample contained no salt, the sample was washed in deionized water and air-dried before analysis. For the samples containing salt, salt solution was prepared by adding NaCl in deionized water to create a saturated salt solution. The salt solution was mixed with the lipid solutions (1:1 volume ratio) and pipetted onto clean silicon wafers and dried at room temperature in a fume hood.

2.2 | Preparation of tissue slices

Tissue samples used for salt addition were rat brain and infarcted mouse hearts. A myocardial infarction was induced in the mouse hearts by a method described elsewhere.[29]

Thin slices of the tissues (6 μm for rat brain and 8 μm for mouse heart) were prepared for ToF-SIMS analysis by cryo-sectioning in an argon-purged cryo-microtome (Leica CM1520, Germany) at −20°C and thaw mounted onto indium tin oxide (ITO)-coated glass microscope slides. The tissue slices were sprayed with a saturated solution of NaCl in methanol using an airbrush supplied with nitrogen gas. The airbrush was optimized so that the methanol would evaporate before hitting the sample causing salt to land evenly on the surface of the sample without wetting the ITO glass slide and tissue section thus minimizing the risk of redistribution of small molecules in the tissue sample.

2.3 | ToF-SIMS analysis

ToF-SIMS analysis was performed using a J105 – 3D Chemical Imager (Ionoptika Ltd, UK) that has been described in detail elsewhere.[2,30] The instrument uses a quasi-continuous primary ion beam to bombard the sample to produce a stream of secondary ions that are bunched to produce a tight packet of ions at the entrance of a reflectron ToF analyser. In this study, a 40 keV gas cluster ion beam was used. Clusters were formed by the expansion of CO_2 (AGA Sweden) into a vacuum chamber at the back of the ion gun that were ionized by electron impact and size selected using a Wien filter.[1]

The spectra of the lipid standards were acquired over a 400 × 400 μm^2 area. The primary ion dose density for each image was 1×10^{13} ions/cm^2. The spectra from the mouse heart tissue sections were acquired over 6 × 6 mm^2 (or 7.2 × 6 mm^2) at a spatial resolution of 20 μm/pixel. The primary ion dose density for each image was 1×10^{12} ions/cm^2. For rat brain tissues sections, the spectra were acquired over 10.8 × 2.4 mm^2 at a spatial resolution of 20 μm/pixel or over 1 × 1 mm^2 at a spatial resolution of 4 μm/pixel. The primary ion dose density for the rat brain images was around 5×10^{12} ions/cm^2. The continuous primary ion current measured into a Faraday cup

was 26 pA. The J105 is fitted with an electron flood gun for charge compensation when needed but was not used in this study.

MS/MS was performed using the J105 as described and demonstrated previously.[2,6,7,20] Briefly, MS/MS was performed in a ToF–ToF configuration with collision-induced dissociation occurring in a short field-free region between the buncher and the reflectron mass analyser where nitrogen gas was injected. Precursor ions have energies in the range 0.5–5 keV depending on their position in the buncher when the bunching voltage was applied. Precursor and corresponding product ions were selected using a timed ion gate at a time focus at the entrance to the mass analyser.

3 | RESULTS AND DISCUSSION

3.1 | Analysis of standards

To study the differences in fragmentation patterns between DAGs and TAGs, two different lipid standards were analysed with and without the addition of salt. The DAG and TAG lipid standards were chosen due to their similar fatty acid content and therefore created similar fragment peaks.

Mass spectra of the chosen DAG and TAG standards without addition of salt are shown in Figure 1. The DAG spectrum shows a strong peak at *m/z* 603.5, assigned to the $[M + H - H_2O]^+$ fragment from the DAG. A smaller $[M + H]^+$ ion at *m/z* 621.5 can also be seen, but at lower abundance than the $[M + H - H_2O]^+$ ion. For TAG, the two major peaks in the spectrum are the DAG-like ions $[M - RCOO]^+$ at *m/z* 577.5 and *m/z* 603.5 due to the loss of either 'R_1COO' or 'R_2COO', respectively. The molecular ion of the TAG $[M + H]^+$ can be found at *m/z* 859.6. The peak at *m/z* 577.5 is the $[M - R_1COO]^+$ ion, where R_1 is the C18:1 species and it is about three times as high as the $[M - R_2COO]^+$ ion at *m/z* 603.5, where R_2 is the C16:0. This is due to the fact that the TAG standard chosen has two fatty acid chains with C18:1 and one fatty acid chain with C16:0. The chance of fragmentation by losing the FA (18:1) is therefore higher than losing a FA (16:0). Inspection of the lower mass region of the spectra (Figure S1, supporting information) shows that the DAG also fragments by loss of RCOO to produce a strong monoacylglyceride (MAG)-like ion at *m/z* 339 that is more intense than the $[M + H - H_2O]^+$. In the TAG spectrum similar ions are detected but in much lower relative abundance. In relatively simple samples the ratio of the MAG/DAG-type ions may provide an indication as to the presence of DAG or TAG molecules but due to many isobaric interferences at this lower mass range it is not likely to be practical for complex biological samples such as cells and tissue.

The TAG $[M - RCOO]^+$ ion is isobaric with the DAG $[M + H - H_2O]^+$ ion, making discrimination of these in biological samples where both DAGs and TAGs might be present impossible without MS/MS, as mentioned above.[20]

Figure 2 shows the DAG region (*m/z* 550–650) of the mass spectra of DAG and TAG standards after addition of salt. When salt is added to the DAG standard a peak at *m/z* 643.5 appears. This new peak, shifted by 40 Da from the $[M + H - H_2O]^+$ ion, is assigned to the sodium adduct of the DAG species $[M + Na]^+$. For the TAG standard, however, the only peaks that are observed in this region are those at *m/z* 577.5 (not shown) and *m/z* 603.5 (the $[M - RCOO]^+$ for the TAG that is isobaric with the $[M + H - H_2O]^+$ for the DAG). No peak at *m/z* 643.5 is detected in the TAG analysis. Hence, by adding salt to the sample, it is possible to differentiate between the DAG and TAG species by the 40 Da peak shift that is only observed for DAGs. If the $[M + Na]^+$ ion is generated, the species originates from a DAG. If no $[M + Na]^+$ is found in the 'DAG' region, the original species is a TAG. Other peaks, in the TAG molecular ion region, that

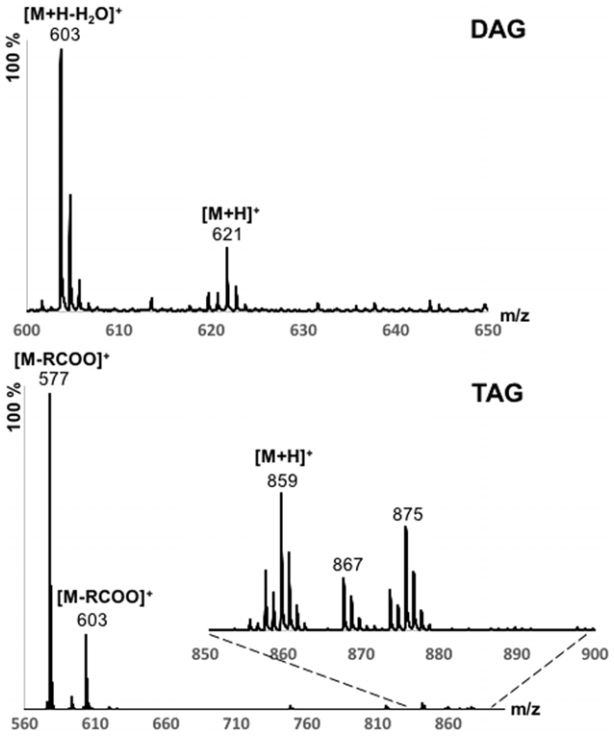

FIGURE 1 Spectra from ToF-SIMS analysis in positive ion mode of a DAG standard (top) and TAG standard (bottom) washed in water using 40 keV $(CO_2)_{6k}^+$ at a primary ion dose of 1×10^{13} ions/cm^2[Color figure can be viewed at wileyonlinelibrary.com]

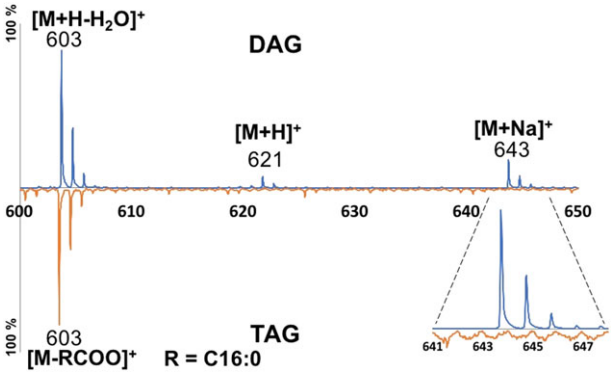

FIGURE 2 Spectra from ToF-SIMS analysis in positive ion mode of a DAG (positive) and TAG (negative) standards, both mixed with a saturated NaCl solution. Zoom-in shows that the *m/z* 643.5 peak is only detected during the DAG analysis. Intensities were normalized to the intensity of the *m/z* 603.5 peak in both spectra. Analysis is done with using 40 keV $(CO_2)_{6k}^+$ ion beam at a primary ion dose of 1×10^{13} ions/cm^2 [Color figure can be viewed at wileyonlinelibrary.com]

can be found in the TAG spectrum are the $[M + H]^+$ and the new $[M + Na]^+$, where the protonated ion is much smaller than the sodiated ion (see Figure S2, supporting information).

3.2 | Applications: analysis of tissues

As SIMS is commonly used in imaging mode for the analysis of biological samples, animal tissue slices were used to further study the use of salt as an approach to determine the origin of different peaks in the mass spectra. Tissue slices were sprayed with a saturated solution of NaCl in methanol (selected instead of water to minimize sample wetting) to create a uniform layer of salt on top of the sample and the differences between the spectra before and after addition of salt were compared. To get an even distribution of salt without wetting the sample, different distances between the sprayer and the sample were tested. If the sample was too close to the sprayer, the NaCl spray wetted the samples, causing lipid species within the sample to migrate (see Figure S3, supporting information). The optimal distance was found when the samples were not wetted by the spray and enough salt was added to the sample to convert most of the peaks to $[M + Na]^+$ ions (see Figure S4, supporting information).

3.2.1 | Mouse heart tissue

The salt spray was applied to mouse heart slices in order to determine the origin of the peaks in the DAG region of the spectra. Salt was applied in a uniform layer with some salt crystal formation on the surface (see overlay image in Figure 5 showing the distribution of the $[K_2Cl]^+$ ion in blue). Potential DAG species were identified at *m/z* 551.5, *m/z* 573.5, *m/z* 599.5 and *m/z* 627.5 and assigned to the DAG-like ions 'DAG'(32:0), 'DAG'(34:3), 'DAG'(36:4) and 'DAG'(38:4), respectively, as shown in Figure 3. No 40 Da shift in peaks was detected upon addition of NaCl. It can also be observed that the DAG-like ions show the same relative intensity pattern both before and after addition of salt, indicating that the peaks originate from fragmentation of TAG species and not DAG species. While no $[M + Na]^+$ DAG ions were observed in the spectrum of the NaCl-treated sample in Figure 3, three additional peaks appear after addition of salt at *m/z* 621.5, *m/z* 645.5 and *m/z* 649.5. These are possibly sodium adducts of chemical species that were of too low abundance to be detected before addition of salt.

In a recent study in our laboratory, mouse hearts were shown to exhibit changes in cation distribution following surgically induced infarction.[29] The sodium level in the damaged/infarcted part of the heart was greater than in the non-infarcted heart tissue, while the potassium levels were greater in the non-infarcted part compared to the damaged/infarcted part as indicated by preferential adduct ion formation of the phosphatidylcholine (PC) lipids. This represents a challenge for interpretation of the mass spectrometry imaging data. The sodiated lipid peaks show accumulation in one part of the heart, whereas the potassiated lipid peaks are correlated to the other part. However, the actual lipid levels may not have changed, only the relative salt levels.[31] For this particular sample, it was hypothesized that the salt addition might provide not only a means to quickly discriminate DAG/TAG fragments, but also to overcome some of the cation-related matrix effect if the Na^+ displaced the K^+. Figure 4 shows mass spectrometry images before and after addition of sodium chloride. The sodiated peaks ($[M + Na - TMA]^+$ and $[M + Na]^+$) of PC (32:0) and PC (34:1) show clear localization to the infarcted region of the heart in the control samples (infarcted region is marked with dashed lines in the images in the first column in Figure 4). TMA is the (59 Da) trimethylamine group at the end of the phospholipid head group. After addition of salt, the distribution of these ions becomes more even over the entire tissue slice. The potassiated ions ($[M + K - TMA]^+$ and $[M + K]^+$) of the same lipids show clear localization to the normal tissue region (non-infarcted region) for the control samples, but after salt addition a more even distribution is found. This

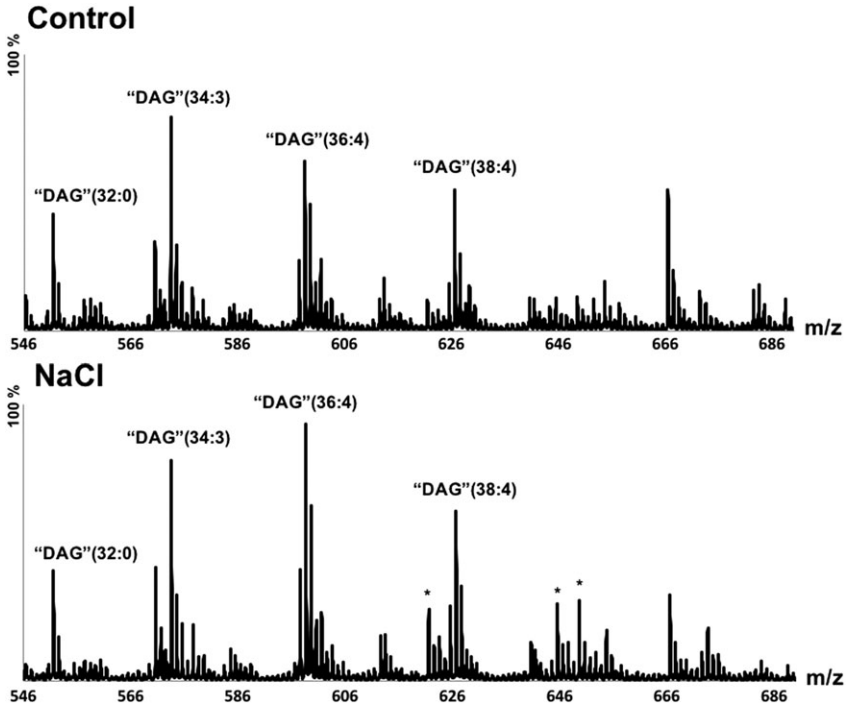

FIGURE 3 Mass spectra of the DAG region from mouse heart samples with (bottom) and without (top) the addition of salt. Asterisks indicate peaks that show increase in the NaCl sample. All the 'DAG'-labelled peaks are $[M + H - H_2O]^+/[M - RCOO]^+$ ions. Intensities are normalized to the number of pixels selected for total area. Analyses were carried out using a 40 keV $(CO_2)_{6k}^+$ ion beam at a primary ion dose of 1×10^{12} ions/cm^2

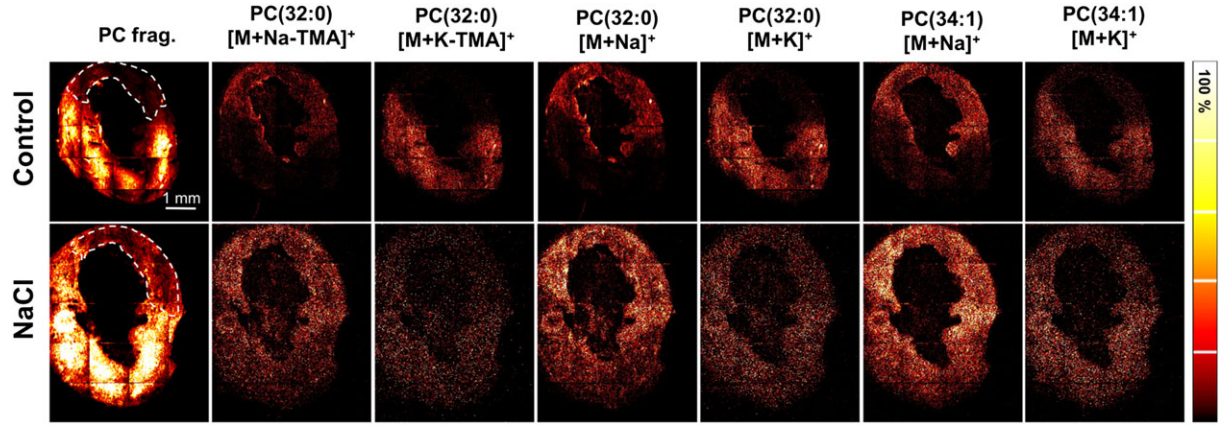

FIGURE 4 Mass spectrometric images of infarcted mouse heart with and without addition of salt. Infarcted areas are shown with dashed lines in images in the first column. Ion images were acquired using a 40 kV $(CO_2)_{6k}^+$ ion beam with primary ion dose density of 1×10^{12} ions/cm^2. All images are 6 mm in width. Scale bar in top left image is 1 mm and applies to all subsequent images. Signal intensity is displayed on a thermal scale as shown on the right [Color figure can be viewed at wileyonlinelibrary.com]

indicates that salt addition can be used in order to overcome some of the differences in cation levels within the tissue during imaging of specific lipid species and improve relative quantification.

An interesting observation was that once the salt effect is reduced, smaller differences in distribution of specific lipids are found that were previously obscured by the larger salt differences. In our previous study, changes in relative saturation states of fatty acids ($[RCOO]^-$ ions) were observed in infarcted heart tissue compared with non-infarcted tissue.[29] These differences in saturation states were not identified for intact PC lipid molecules in positive ion mode as the huge differences arising from different cationization masked these subtleties. Once salt was added, differences in distribution between differently saturated lipids with the same number of carbons became apparent (see Figure 5). The mass spectrometric image of *m/z* 780.6 (PC (34:2), $[M + Na]^+$) shows higher intensity in the infarcted region than the more saturated species at *m/z* 782.6 (PC (34:1), $[M + Na]^+$), which is more evenly distributed across the heart tissue. The completely saturated species PC (34:0), $[M + Na]^+$, at *m/z* 784.6, shows even stronger correlation to the infarcted region. The same is observed for the species at *m/z* 808.6 (PC (36:2), $[M + Na]^+$) and *m/z* 810.6 (PC (36:1), $[M + Na]^+$), which shows that the less saturated lipids are correlated to the infarcted region. The completely saturated species at *m/z* 812.6 (PC (36:0), $[M + Na]^+$) is highly localized to the infarcted region. These results are in agreement with a previous study of infarcted mouse hearts where the saturated fatty acids were correlated with the infarction region, and it was hypothesized to be due to disruption of the normal β-oxidation processes in the tissue during infarction.[29] The differences in distribution observed between intact lipid species with one and two double bonds were, however, not identified previously.

3.2.2 | Brain tissue

Salt was applied to rat brain tissue similarly to the heart tissue, in order to determine the origin of the DAG-like ions in the spectra from the brain. Salt was successfully added as a uniform layer on top of the

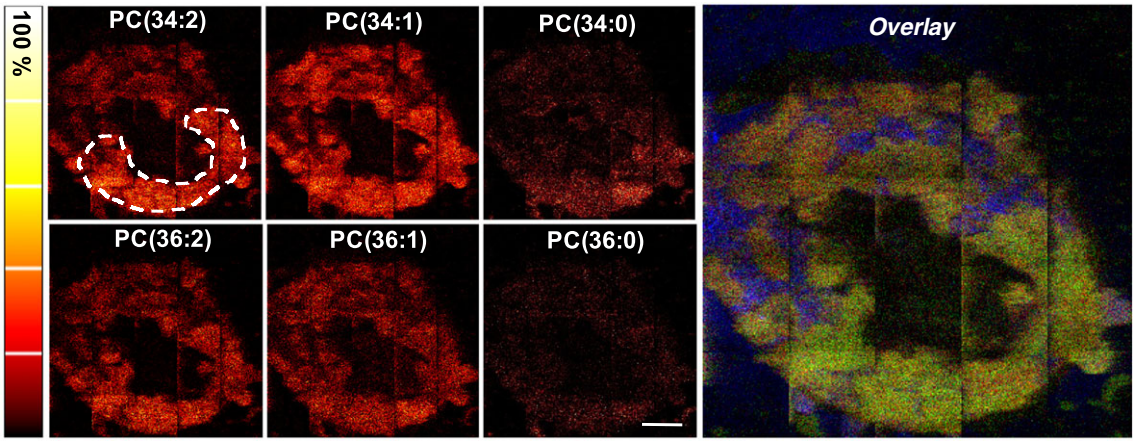

FIGURE 5 Mass spectrometric images of infarcted mouse heart after addition of salt. Infarcted area is shown with dashed lines in the first image. Overlaid image shows *m/z* 780.6 (PC (34:2)) in green, *m/z* 782.6 (PC (34:1)) in red and *m/z* 112.9 (K_2Cl) in blue. Ion images were acquired using a 40 kV $(CO_2)_{6k}^+$ ion beam with primary ion dose density of 1×10^{12} ions/cm^2. All images are 6 mm in width. Scale bar in top left image is 1 mm and applies to all subsequent single ion images. Signal intensity is displayed on a thermal scale as shown on the left [Color figure can be viewed at wileyonlinelibrary.com]

brain slices, which is shown in Figure S5 (supporting information). Inspection of the control brain mass spectrometry images does not show any formation of salt crystals on top of the tissue. On the slices where salt was added, salt signals were detected at *m/z* 80.9, $[Na_2Cl]^+$, and *m/z* 112.9, $[K_2Cl]^+$, suggesting some crystal formation on the tissue. Figure S4 (supporting information) shows the difference between the spectra from brain samples with and without the addition of salt. ToF-SIMS analysis of rat brain shows strong spectral differences between the grey and white matter regions of the brain with the white matter regions dominated by a strong cholesterol signal due to migration of this species during sample preparation and exposure to the vacuum environment of the mass spectrometer. This is an effect that is removed by frozen hydrated analysis or trifluoroacetic acid.[32,33] For this reason, in the comparison shown here, signal was extracted from predominantly grey matter areas of the tissue. To account for small differences in the amount of white/grey matter included in the comparison spectra the signals were normalized using the cholesterol peak at *m/z* 369.3. The control brain spectrum (top spectrum in Figure S4, supporting information) is dominated by potassiated ions, such as $[M + K]^+$ and $[M - TMA + K]^+$. After application of NaCl by spraying, the majority of the peaks shift towards the $[M + Na]^+$ and the $[M - TMA + Na]^+$ peaks (bottom spectrum in Figure S4) confirming successful salt addition to the sample.

In Figure 6, the spectra from the DAG region are shown for the rat brain before and after the addition of NaCl. Peaks are observed at *m/z* 551.5, *m/z* 571.5, *m/z* 573.5, *m/z* 577.5, *m/z* 599.5, *m/z* 605.5 and *m/z* 627.5 and assigned to the DAG-like ions 'DAG'(32:0), 'DAG'(34:4), 'DAG'(34:3), 'DAG'(34:1), 'DAG'(36:4), 'DAG'(36:1) and 'DAG'(38:4), respectively. The top spectrum shows the peaks from the control samples, without the addition of salt. When adding salt, some peaks disappear from the spectrum (peaks marked with asterisks in top spectrum in Figure 3). MS/MS analysis of the disappearing peaks (control tissue section) showed that they originate from potassiated ions. After addition of salt the potassiated peaks are no longer observed and sodiated peaks (−16 *m/z*) are detected instead, as observed in the spectrum of the intact lipid region. The peaks at *m/z* 551.5, *m/z* 571.5, *m/z* 573.5, *m/z* 577.5, *m/z* 605.5 and *m/z* 627.5 do not change relative to each other between the sample with salt and the control sample. Since no shift was observed and no new peaks 40 Da higher were detected, we conclude that the peaks belong to $[M - RCOO]^+$ fragments of TAG species and not $[M + H - H_2O]^+$ ions of DAGs.

During analysis of the heart tissue, the peak at *m/z* 599.5 increased in height after addition of NaCl (see Figure 3). MS/MS analysis of this peak identifies this species as a sodiated ion, which explains why the peak is higher after salt addition. Usually the *m/z* 599.5 peak is assigned as a $[M + H - H_2O]^+$ fragment of a DAG species, but since this peak is enhanced after addition of salt we now suspect that there is a previously unreported isobaric interference at this *m/z* value, one DAG-like ion and one sodiated lipid species. In Figure 6, a peak at *m/z* 615.5 is observed in the control brain tissue sample spectrum but not in the NaCl-treated sample spectrum. This is likely a potassiated ion that after salt addition is replaced by a sodiated ion causing the peak to shift to *m/z* 599.5.

4 | CONCLUSIONS

By addition of salt to the surface of lipid samples, new information about the different samples analysed can be identified and the method has been shown to be helpful for interpretation of complex mass spectra for two different kinds of tissues, heart and brain. The SIMS fragmentation pattern differs between DAGs and TAGs in the presence of salt and can be used to determine the origin of the species. Only DAGs form the sodiated ion so this peak can confirm the presence of DAGs in samples including those containing combinations of DAGs and TAGs. At present, we do not have a way of determining the relative abundance of DAG versus TAG in mixed samples as in such cases the isobaric DAG-like ions will still be present along with the adduct ions. Our analysis reveals that all the DAG-like ions we identify in the spectra, from both types of tissues, originate from TAG species that have fragmented into DAG-like ions during the ionization process. This has been hypothesized for SIMS data based on the relative

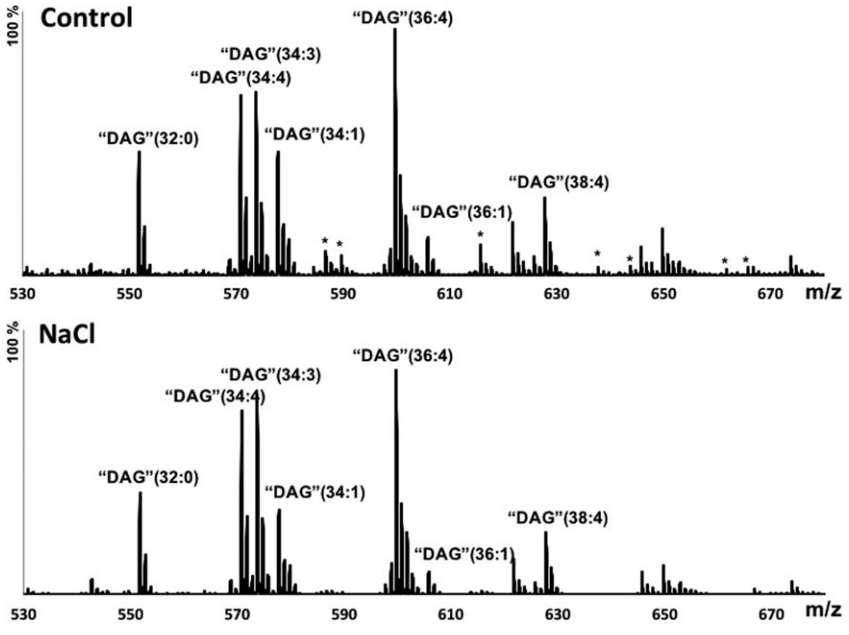

FIGURE 6 Mass spectra of the DAG region from rat brain samples with (bottom) and without (top) the addition of salt. Asterisks indicate peaks that were only found in the control sample. All the 'DAG'-labelled peaks are $[M + H - H_2O]^+/[M - RCOO]^+$ ions. Intensities are normalized to the number of pixels selected in the image and the cholesterol peak at *m/z* 369.3. Analysis was done using a 40 keV $(CO_2)_{6k}^+$ ion beam at a primary ion dose of 5×10^{12} ions/cm^2

biological abundance of the two lipid classes,[21-23] but never clearly demonstrated. MS/MS analysis of the brain tissue as well as liquid chromatography–MS analysis of the infarcted heart tissue also showed that the peaks are more likely fragmentation ions from TAG (see Figures S6 and S7, supporting information). The method could also be used to identify the peaks that are salt adducts without the need for using MS/MS, which is often not available in most ToF-SIMS laboratories. Further, salt addition might be used as a way of minimizing the differences in salt levels within infarcted hearts or similar samples that have been shown to exhibit differences in Na^+ and K^+ levels across the tissue matrix. When the differences in cation concentration are diminished, smaller differences masked under the salt differences are found, such as differences in saturation levels between infarcted and non-infarcted areas.

ACKNOWLEDGEMENTS

The imaging mass spectrometry experiments were performed at Go:IMS at the University of Gothenburg and Chalmers University of Technology in Gothenburg, Sweden. The authors thank Marwa Munem and Amir Saeid Mohammadi (University of Gothenburg) for constructive comments and help in slicing of rat brains, respectively. Also, we thank Jan Borén (Wallenberg Centre for Cardiovascular Research, University of Gothenburg) for collaboration on the mouse heart study and providing liquid chromatography–MS data. The authors also acknowledge financial support from the Swedish Research Council, the Knut and Alice Wallenberg Foundation and the National Institutes of Health.

ORCID

John S. Fletcher http://orcid.org/0000-0002-9418-8571

REFERENCES

1. Angerer TB, Blenkinsopp P, Fletcher JS. High energy gas cluster ions for organic and biological analysis by time-of-flight secondary ion mass spectrometry. *Int J Mass Spectrom*. 2015;337:591-598.
2. Fletcher JS, Rabbani S, Henderson A, et al. A new dynamic in mass spectral imaging of single biological cells. *Anal Chem*. 2008;80(23):9058-9064.
3. Smith DF, Robinson EW, Tolmachev AV, Heeren RMA, Pasa-Tolic L. C-60 secondary ion Fourier transform ion cyclotron resonance mass spectrometry. *Anal Chem*. 2011;83(24):9552-9556.
4. Passarelli MK, Pirkl A, Moellers R, et al. The 3D OrbiSIMS-label-free metabolic imaging with subcellular lateral resolution and high mass-resolving power. *Nat Methods*. 2017;14(12):1175-1183.
5. Gilmore IS, Green FM, Seah MP. Static TOF-SIMS. A VAMAS interlaboratory study. Part II: accuracy of the mass scale and G-SIMS compatibility. *Surf Interface Anal*. 2007;39(10):817-825.
6. Fletcher JS, Kotze HL, Armitage EG, Lockyer NP, Vickerman JC. Evaluating the challenges associated with time-of-fight secondary ion mass spectrometry for metabolomics using pure and mixed metabolites. *Metabolomics*. 2013;9(3):535-544.
7. Wehrli PM, Lindberg E, Angerer TB, et al. Maximising the potential for bacterial phenotyping using time-of-flight secondary ion mass spectrometry with multivariate analysis and tandem mass spectrometry. *Surf Interface Anal*. 2014;46:173-176.
8. Baig NF, Dunham SJB, Morales-Soto N, et al. Multimodal chemical imaging of molecular messengers in emerging *Pseudomonas aeruginosa* bacterial communities. *Analyst*. 2015;140(19):6544-6552.
9. Fisher GL, Bruinen AL, Potocnik NO, et al. A new method and mass spectrometer design for TOF-SIMS parallel imaging MS/MS. *Anal Chem*. 2016;88(12):6433-6440.
10. Carrasco S, Mérida I. Diacylglycerol, when simplicity becomes complex. *Trends Biochem Sci*. 2007;32(1):27-36.
11. Shemesh T, Luini A, Malhotra V, Burger KNJ, Kozlov MM. Prefission constriction of Golgi tubular carriers driven by local lipid metabolism: a theoretical model. *Biophys J*. 2003;85(6):3813-3827.
12. Yang C, Kazanietz MG. Divergence and complexities in DAG signaling: looking beyond PKC. *Trends Pharmacol Sci*. 2003;24(11):602-608.
13. Brose N, Betz A, Wegmeyer H. Divergent and convergent signaling by the diacylglycerol second messenger pathway in mammals. *Curr Opin Neurobiol*. 2004;14(3):328-340.
14. Zhang L, Ussher JR, Oka T, et al. Cardiac diacylglycerol accumulation in high fat-fed mice is associated with impaired insulin-stimulated glucose oxidation. *Cardiovasc Res*. 2011;89(1):148-156.
15. Housey GM, Johnson MD, Hsiao WL, et al. Overproduction of protein kinase C causes disordered growth control in rat fibroblasts. *Cell*. 1988;52(3):343-354.
16. Sharma S, Adrogue JV, Golfman L, et al. Intramyocardial lipid accumulation in the failing human heart resembles the lipotoxic rat heart. *FASEB J*. 2004;18(14):1692-1700.
17. Brindley DN. Metabolism of triacylglycerols. In: Vance DE, Vance JE, eds. *New Comprehensive Biochemistry*. Vol.20 Amsterdam: Elsevier; 1991:171-203.
18. Voet D. Lipids and membranes. In: Voet D, Voet JG, eds. *Biochemistry*. New York, NY: Wiley; 1990;386-466.
19. Farese RV, Walther TC. Lipid droplets finally get a little R-E-S-P-E-C-T. *Cell*. 2009;139(5):855-860.
20. Phan NTN, Munem M, Ewing AG, Fletcher JS. MS/MS analysis and imaging of lipids across Drosophila brain using secondary ion mass spectrometry. *Anal Bioanal Chem*. 2017;409(16):3923-3932.
21. Hayakawa J, Wang M, Wang C, et al. Lipidomic analysis reveals significant lipogenesis and accumulation of lipotoxic components in ob/ob mouse organs. *Prostaglandins Leukot Essent Fatty Acids*. In press. doi: https://doi.org/10.1016/j.plefa.2017.01.002
22. Arner P, Östman J. Mono- and diacylglycerols in human adipose tissue. *Biochim Biophys Acta (BBA)*. 1974;369(2):209-221.
23. Kennerly DA, Parker CW, Sullivan TJ. Use of diacylglycerol kinase to quantitate picomole levels of 1,2-diacylglycerol. *Anal Biochem*. 1979;98(1):123-131.
24. Harvey DJ. Matrix-assisted laser desorption/ionization mass spectrometry of phospholipids. *J Mass Spectrom*. 1995;30(9):1333-1346.
25. Asbury GR, Al-Saad K, Siems WF, Hannan RM, Hill HH. Analysis of triacylglycerols and whole oils by matrix-assisted laser desorption/ionization time of flight mass spectrometry. *J Am Soc Mass Spectrom*. 1999;10(10):983-991.
26. Al-Saad KA, Zabrouskov V, Siems WF, et al. Matrix-assisted laser desorption/ionization time-of-flight mass spectrometry of lipids: ionization and prompt fragmentation patterns. *Rapid Commun Mass Spectrom*. 2003;17(1):87-96.
27. Gidden J, Liyanage R, Durham B, Lay JO. Reducing fragmentation observed in the matrix-assisted laser desorption/ionization time-of-flight mass spectrometric analysis of triacylglycerols in vegetable oils. *Rapid Commun Mass Spectrom*. 2007;21(13):1951-1957.
28. Al-Saad KZV, Siems W, Knowles N, Hannan R, Hill H Jr. Matrix-assisted laser desorption/ionization time-of-flight mass spectrometry of lipids: ionization and prompt fragmentation patterns. *Rapid Commun Mass Spectrom*. 2003;17(1):87-96.
29. Sämfors S, Ståhlman M, Klevstig M, Borén J, Fletcher JS. Localised lipid accumulation detected in infarcted mouse heart tissue using ToF-SIMS. *Int J Mass Spectrom*. In press. doi: https://doi.org/10.1016/j.ijms.2017.09.012

30. Hill R, Blenkinsopp P, Thompson S, Vickerman J, Fletcher JS. A new time-of-flight SIMS instrument for 3D imaging and analysis. *Surf Interface Anal*. 2011;43(1–2):506-509.

31. Lanekoff I, Stevens SL, Stenzel-Poore MP, Laskin J. Matrix effects in biological mass spectrometry imaging: identification and compensation. *Analyst*. 2014;139(14):3528-3532.

32. Angerer TB, Dowlatshahi Pour M, Malmberg P, Fletcher JS. Improved molecular imaging in rodent brain with time-of-flight-secondary ion mass spectrometry using gas cluster ion beams and reactive vapor exposure. *Anal Chem*. 2015;87(8):4305-4313.

33. Angerer TB, Mohammadi AS, Fletcher JS. Optimizing sample preparation for anatomical determination in the hippocampus of rodent brain by ToF-SIMS analysis. *Biointerphases*. 2016;11(2):02A319.

SUPPORTING INFORMATION

Additional supporting information may be found online in the Supporting Information section at the end of the article.

How to cite this article: Sämfors S, Ewing AG, Fletcher JS. Benefits of NaCl addition for time-of-flight secondary ion mass spectrometry analysis including the discrimination of diacylglyceride and triacylglyceride ions. *Rapid Commun Mass Spectrom*. 2018;32:1473–1480. https://doi.org/10.1002/rcm.8181